Strain-engineered photoluminescence of silicon nanoclusters

X.-H. Peng,[1,2] S. Ganti,[2] A. Alizadeh,[2] P. Sharma,[3] S. K. Kumar,[4] and S. K. Nayak[1]
[1]*Department of Physics, Applied Physics and Astronomy, Rensselaer Polytechnic Institute, Troy, New York 12180, USA*
[2]*General Electric Global Research Center, Niskayuna, New York 12309, USA*
[3]*Department of Mechanical Engineering, Department of Physics, University of Houston, Houston, Texas 77204, USA*
[4]*Department of Chemical and Biological Engineering, Rensselaer Polytechnic Institute, Troy, New York 12180, USA*
(Received 22 May 2006; published 27 July 2006)

Density functional calculations on silicon clusters show that strain effects on the band gap display qualitatively new trends for dots smaller than ~2 nm. While the bulk indirect band gap increases linearly with increasing strain, this trend is reversed for small clusters (≤1 nm). In the intermediate 1–2 nm size range, strain appears to have almost no effect. These results follow from the fact that the bonding/antibonding character of the HOMO and the LUMO change nonmonotonically with size. Since the strain level of the surface atoms dominate this behavior, they strongly stress the role of surface passivation on experimentally measured band gaps.

DOI: 10.1103/PhysRevB.74.035339 PACS number(s): 78.55.−m, 71.15.Mb, 73.22.Dj, 78.67.Bf

The decrease in size of semiconductor nanoclusters can result in a variety of new properties that are absent in the bulk. For example, while bulk silicon does not emit visible light, photoluminescence is found for clusters smaller than a critical dimension.[1–4] This effect is ascribed to strong quantum confinement. In addition, the band gap in silicon quantum dots has been shown to substantially vary through surface passivation,[5–8] i.e., oxygen and other double bonded atoms have a dramatic effect as compared to hydrogenated clusters. Passivation with single bonded atoms, however, has minimal impact. These findings have led to the possibility of using silicon dots in technological applications ranging from optoelectronic devices to biological labels.[9,10]

Several *experiments* have studied the role of strain and quantum confinement on optical emission. Examples include strained silicon dots (with size larger than 2 nm) embedded in a silicon dioxide matrix,[11,12] and InAs dots embedded in $In_xGa_{1-x}As$ confining layers: the strain in this case is controlled by varying the In composition of the confining layers.[13,14] In addition, Buda and Aparisi *et al.*[15,16] studied the electronic and optical properties of III–V and II–VI semiconductor clusters encapsulated in the zeolites (and sodalite) cage and observed the shift of the energy gap of the semiconductor clusters due to resultant tensile/compressive strain exerted by the cage on the clusters. While these works find evident strain effects on the band gap, to our knowledge no theoretical study has focused on the coupled effects of size and strain in the case of semiconductor nanodots. This work bridges this gap, especially focusing on the sub-2 nm size range, where we predict that new, interesting phenomena will occur.

We have studied the energy gap (EG) of silicon clusters containing up to $Si_{123}H_{100}$ (~1.7 nm diameter) using several computational tools. The starting atomic coordinates for these clusters are obtained from bulk silicon (lattice constant of 0.5461 nm). The dangling bonds of the surface silicon atoms are terminated by hydrogen at an initial bond length of 0.147 nm. The structure of the cluster is then relaxed using the energy minimization technique. The atomic and electronic structure of these clusters are computed via density functional theory (DFT) based on the generalized gradient approximation (GGA) using the Perdew-Wang 91 (PW91) functional.[17] The pseudopotential plane wave approach with super cell method is utilized.[18] Note that the super cell size, 3 nm on a side, is large enough that each nanocluster was surrounded by at least 1.2 nm of empty space—the interaction between replicas is thus minimized. The interaction between ions and electrons is described by ultrasoft Vanderbilt pseudopotentials. The kinetic energy cutoff for the plane wave basis set is 300 eV corresponding to about 10^6 plane waves. The EG of a given cluster is computed from the difference between the eigenvalues of the highest occupied molecular orbital (HOMO) and the lowest unoccupied molecular orbital (LUMO). DFT was originally developed for the ground state, and it is well known to underestimate the EG. While this effect might be corrected by excited state calculations,[19–21] we will focus on the DFT predictions of HOMO-LUMO gaps which should provide qualitatively accurate predictions of the relative change in the EG with strain. In fact, we have compared our DFT results with more accurate calculations and have confirmed our conclusion obtained from the DFT method (see below).

The variation of the EG with size for relaxed silicon clusters (Fig. 1) is in good agreement with previous studies.[2,4,22] The small but noticeable difference between various studies is due to the different methods and functionals used. The optimized unstrained nanoclusters were isotropically strained up to ±8% by rescaling atom positions. The positive values of strain refer to expansion, while negative corresponds to compression (although these results are for structures which are not further optimized, below we show that different means of equilibrating them play a minor role). Note that the strain extremes are beyond the elastic limit in bulk silicon. However, the nucleation of defects (e.g., dislocations and disclinations) becomes energetically unfavorable especially in small clusters, and is hence improbable. The change of band gap as a function of strain in silicon is shown in Figs. 2(a)–2(d). One notices that the bulk indirect band gap increases almost linearly with increasing strain—this result is in good agreement with earlier studies and corresponds to a constant deformation potential parameter.[23] In contrast, the strain dependence of the smallest cluster (Si_5H_{12}) shows the

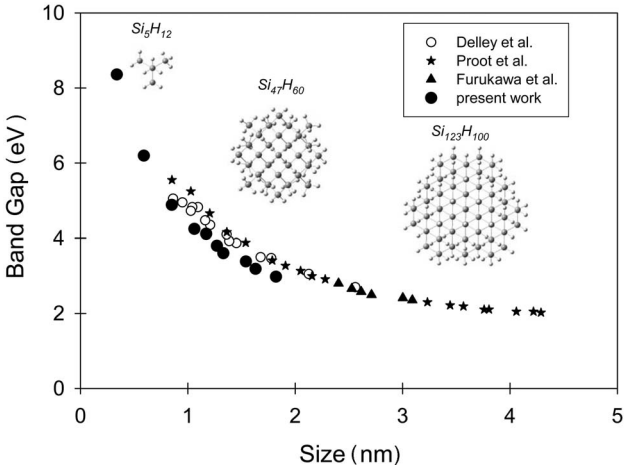

FIG. 1. Variation of the energy gap as a function of Si cluster size. Similar to previous studies (Ref. 2), the self-energy correction scheme has been applied to the computed band gap by adding a constant value 0.6 eV. Atomic structures are shown in the inset for several clusters. (●) Present work, (○) Delley *et al.* (Ref. 2), (★) Proot *et al.* (Ref. 4), (▲) Furukawa *et al.* (Ref. 22).

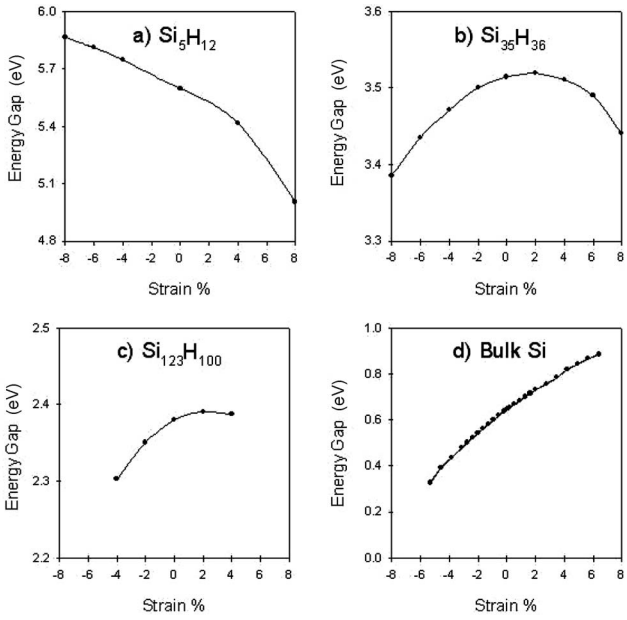

FIG. 2. HOMO-LUMO gap as a function of strain for different size Si clusters and bulk. Positive strain refers to expansion of a cluster while negative strain corresponds to its compression.

opposite dependence. Clusters which are 1–2 nm in size show intermediate behavior. Note that the overall change in the EG with strain is rather small in this intermediate regime. Additionally, the EG decreases both with compressive and expansive strains, exhibiting an approximately parabolic behavior.

We next examine the accuracy of the DFT predictions of the unusual strain effects. First, to involve the exciton Coulomb interaction, we perform configuration interaction singles (CIS) (Ref. 24) calculations. The optical gap in CIS is defined as the excitation energy of the lowest dipole-allowed electronic transition. The strain dependent trends of optical gaps for Si_5H_{12}, $Si_{17}H_{36}$, and $Si_{35}H_{36}$ clusters are in good agreement with the DFT predictions of the HOMO-LUMO gaps [Fig. 3(a)]. Second, we calculate the "quasiparticle gap" as the difference of ionization potential (energy needed to remove an electron from the system) and electron affinity (energy required to add an extra electron to the system). These calculations are performed using the cluster approach with the all electron basis set 6-31+G* (Ref. 25) in order to avoid the Ewald summation in charged clusters that arise in the periodic super cell method. These calculation steps are repeated at different strains for $Si_{35}H_{36}$ clusters. The trends obtained from DFT are in excellent agreement with those computed directly from the super-cell and CIS methods [Fig. 3(b)] giving us additional confidence in our results.

Recently, Draeger *et al.* found that the EG of a $Si_{29}H_{36}$ cluster[26] was practically insensitive to tensile strain in the ranges considered here. While this result for one cluster size is consistent with our findings, we emphasize that no work to date has studied the coupled effects of size and strain on the EG.

Replotting the data in Fig. 2 yields three different regimes of strain-EG dependence (Fig. 4). In regime I (clusters smaller than 1 nm), tensile strain results in a significant reduction of the EG. Compression yields an opposite trend. In regime II (cluster size ~1–2 nm), the EG is effectively insensitive to strain. Finally, in regime III (>2 nm), bulklike behavior results—tension increases the EG. These results are understood as follows. From a continuum perspective, the predominant effect of hydrostatic strain is to shift energy levels and these changes are related to the deformation po-

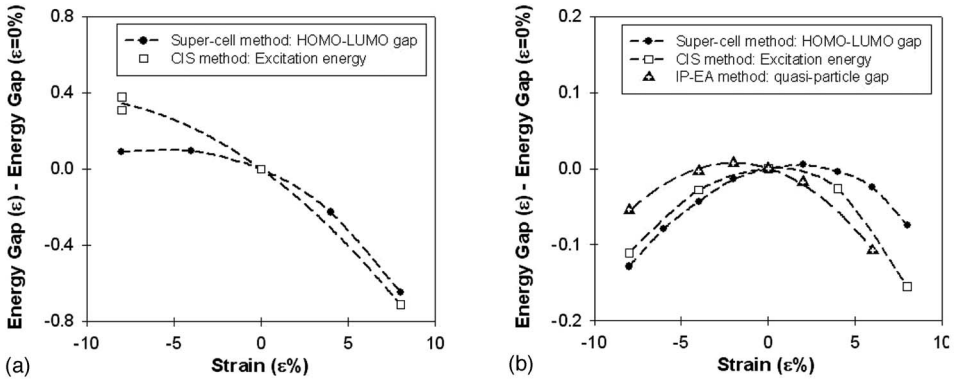

FIG. 3. Comparison of the energy gap simulated by different methods. (●) DFT HOMO-LUMO gap, (□) the excitation energy between the ground state and the lowest dipole-allowed exited state by CIS, (△) the quasiparticle gap defined as the difference of IP and EA. (a) Cluster $Si_{17}H_{36}$ and (b) Cluster $Si_{35}H_{36}$.

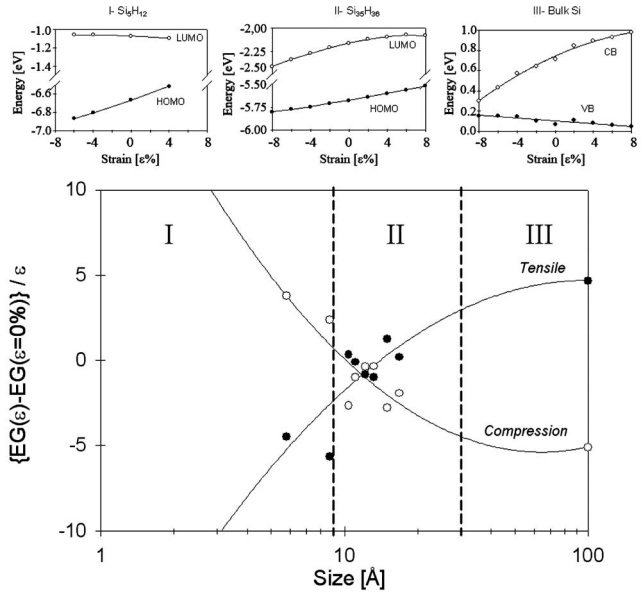

FIG. 4. Map of the strain-energy gap coupling for different size clusters. The *Y*-axis corresponds to the rate of energy gap change with strain, which is defined as the strain normalized difference between the energy gaps of strained and relaxed clusters. Filled symbols correspond to a 4% tensile strain, while hollow symbols represent a 4% compressive strain. Based on the cluster size, three regimes of behavior can be identified. The inset figures illustrate the HOMO-LUMO variation as a function of strain in each of these regimes.

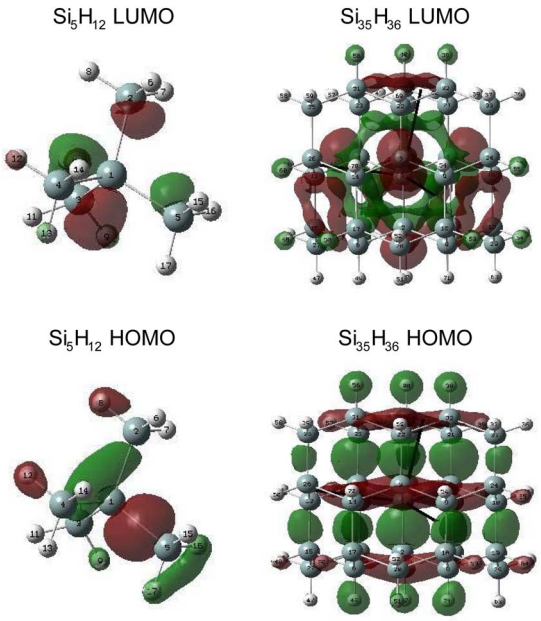

FIG. 5. (Color online) HOMO and LUMO for Si_5H_{12} and $Si_{35}H_{36}$ clusters. HOMO and LUMO electron density contour plots are at the same numerical value in the same species. The structures show strong bonding characters in HOMO. Antibonding feature of LUMO is dominated in Si_5H_{12}, while the LUMO of $Si_{35}H_{36}$ includes a certain mixture of bonding and antibonding characters.

tentials. The band gap of a strained semiconductor can be expressed as EG $\sim \Delta a * \varepsilon$, where $\Delta a = a_c - a_v$. ε is the trace of the strain tensor and a_c and a_v correspond to the deformation potentials for the conduction and the valence band, respectively. Although the concept of a deformation potential is ill defined for such small sizes, it is nevertheless a useful concept to interpret our results. As shown in Fig. 4, the a_v (the deformation potential for HOMO) is large compared to a_c (the deformation potential for LUMO) for small clusters. The electron density contour plots of HOMO and LUMO for Si_5H_{12} at a fixed value (Fig. 5) illustrate that the HOMO has a bonding character: that is, the electron cloud is mainly located in the intermediate regions shared by silicon atoms. In contrast, the LUMO has an antibonding character, i.e., the charge density primarily distributes in the vicinity of atoms (the characteristics of HOMO and LUMO are in excellent agreement with previous work[21]). The reduction of Si-Si bond lengths on compression make the electron cloud of HOMO more efficiently shared by Si atoms. This results in an appreciable decrease of the HOMO energy due to the increased electron-nucleus attraction (the change in the electron-electron repulsion energy is relatively small). In the case of LUMO, the strain effect is small as electrons are already localized in the neighborhood of the atoms. (Note that the effect of nuclei-nuclei interaction is taken as a constant shift in the total energy—this is not included in the calculation of electronic orbital energies.) In intermediate size clusters, LUMO also acquires a level of bonding character in addition to its inherent antibonding nature (see Fig. 5). Consequently, both LUMO and HOMO are similarly affected by strain (Fig. 4), thus resulting in a negligible change in the EG. The bulklike behavior is fully expected. As empirical models (such as the standard 8×8 *kp* approach) indicate, the strain-band gap coupling is linear (i.e., the deformation potential parameter is a constant). The valence band, due to its *p*-type symmetry, does not exhibit a major shift thus contributing little to strain induced band gap changes. On the other hand, the conduction band shows a large shift. This is fully reflected in the larger (empirical) conduction band deformation potential constants as compared to the valence band deformation constants.[27]

In addition to the size dependence of the EG, other electronic properties, such as the nature of quantum transition (dipole allowed or forbidden) also asymptotically approach those of bulk silicon with increasing cluster size.[2,28] To make contact with the experimentally measured photoluminescence intensity we compute the dipole oscillator strength of the energy gap transition by the CIS method. The excited state corresponds to the configuration constituted by moving one electron from HOMO to LUMO. In Table I, the oscillator strengths of the transition for several clusters at different strain levels are presented. The oscillator strength decreases when compressive strain is applied, while the reverse trend follows for tensile strain. Since the exciton lifetimes are inversely proportional to the oscillator strength, our results could be exploited for the accurate determination of underlying strain in small clusters deposited on surfaces or clusters isolated in matrices.

In the preceding results, strain was applied by rescaling all the atomic coordinates. This corresponds to an isotropic strain situation. In experiments, applying such strain to small

TABLE I. The variation of the oscillator strength with strain for several clusters.

	Strain (%)	Excitation energy (eV)	Oscillator strength
	−8	7.38	0.4449
Si_5H_{12}	0	6.98	0.5464
	8	5.95	0.5807
	−8	5.58	0.0278
$Si_{17}H_{36}$	0	5.27	0.1438
	8	4.56	0.7754
	−8	4.37	0.0052
$Si_{35}H_{36}$	0	4.48	0.0082
	8	4.33	0.1112

clusters is challenging. In order to test for the robustness of these conclusions, we have tried different means of strain application. First, we applied a uniform strain to the surface atoms: the internal atoms were either initially strained and fixed, or allowed to equilibrate in response to the surface. Virtually identical strain-EG curves were obtained for all these cases for two cluster sizes, $Si_{35}H_{36}$ and $Si_{87}H_{76}$. We have also used different strain levels for the surface and for the core: in these cases the results virtually converged to the isotropic cases discussed above, but for strain values corresponding to the surface. We find while strain field experienced by the surface atoms modify both HOMO and LUMO energy, the core atoms serving to only slightly modify the LUMO (while playing no role at all in the HOMO). These results stress the fact that the dominant effect arises from the surface, and that the mode of application of strain to the internal core atoms only plays a secondary role. They also allow us to critically understand the large role played by surface passivation on the EG. It is important to note that we have in essence only attempted to impose effectively isotropic strain fields on the dots. This is unlikely to be realistic in the context of experiments, where strains likely are anisotropic. This work thus should be viewed as a first step in understanding more complicated situations.

In summary, we have investigated the size-dependence of the strain-EG coupling in small Si clusters and found qualitatively new behavior in the sub-2 nm size-regime. Recently it is possible to synthesize and probe the electronic properties of ultra-small silicon clusters (less than 2 nm)[29,30] and it will be interesting to verify our predictions of strain effect on the energy gap of small silicon clusters. Our results suggest that simple combinations of size and strain permit the engineering of the photoluminescence of silicon clusters. This offers the possibility of designing novel classes of optical devices and chemical sensors, which exploit these coupled effects.

Financial support from NSF GOALI No. CTS-0327981 is acknowledged. We thank NCSA for providing the computational resources, and M. L. Blohm and the Nanotechnology Program at GE Global Research Center for partial financial support. P.S. would like to acknowledge partial support from ONR No. N000140510662. F. Tang, K. Iyakutti, N. Bhate, and J-U. Lee are acknowledged for helpful discussions.

[1] L. T. Canham, Appl. Phys. Lett. **57**, 1046 (1990).
[2] B. Delley and E. F. Steigmeier, Phys. Rev. B **47**, 1397 (1993); Appl. Phys. Lett. **67**, 2370 (1995).
[3] L.-W. Wang and A. Zunger, J. Chem. Phys. **100**, 2394 (1994).
[4] J. P. Proot, C. Delerue, and G. Allan, Appl. Phys. Lett. **61**, 1948 (1992); C. Delerue, M. Lannoo, and G. Allan, Phys. Rev. Lett. **84**, 2457 (2000).
[5] M. V. Wolkin, J. Jorne, P. M. Fauchet, G. Allan, and C. Delerue, Phys. Rev. Lett. **82**, 197 (1999).
[6] A. Puzder, A. J. Williamson, J. C. Grossman, and G. Galli, Phys. Rev. Lett. **88**, 097401 (2002); Mater. Sci. Eng., B **96**, 80 (2002); J. Chem. Phys. **117**, 6721 (2002).
[7] Z.-Y. Zhou, L. Brus, and R. Friesner, Nano Lett. **3**, 163 (2003).
[8] T. Shimizu-Iwayama, D. E. Hole, and I. W. Boyd, J. Phys.: Condens. Matter **11**, 6595 (1999).
[9] K. D. Hirschman, L. Tsybeskov, S. P. Duttagupta, and P. M. Fauchet, Nature (London) **384**, 338 (1996).
[10] L. Pavesi, L. Dal Negro, C. Mazzoleni, G. Franzo, and F. Priolo, Nature (London) **408**, 440 (2000).
[11] A. Thean and J. P. Leburton, Appl. Phys. Lett. **79**, 1030 (2001).
[12] X. L. Wu and F. S. Xue, Appl. Phys. Lett. **84**, 2808 (2004).
[13] L. Seravalli, M. Minelli, P. Frigeri, P. Allegri, V. Avanzini, and S. Franchi, Appl. Phys. Lett. **82**, 2341 (2003).
[14] S. Mazzucato, D. Nardin, M. Capizzi, A. Polimeni, A. Frova, L. Seravalli, and S. Franchi, Mater. Sci. Eng., C **25**, 830 (2005).
[15] F. Buda and A. Fasolino, Phys. Rev. B **60**, 6131 (1999).
[16] A. Aparisi, V. Fornés, F. Márquez, R. Moreno, C. López, and F. Meseguer, Solid-State Electron. **40**, 641 (1996).
[17] K. Burke, J. P. Perdew, and Y. Wang, in *Electronic Density Functional Theory: Recent Progress and New Directions*, edited by J. F. Dobson, G. Vignale, and M. P. Das (Plenum, New York, 1998).
[18] G. Kresse and J. Furthmüller, Phys. Rev. B **54**, 11169 (1996); G. Kresse and J. Furthmuller, Comput. Mater. Sci. **6**, 15 (1996).
[19] L. Hedin, Phys. Rev. **139**, A796 (1965).
[20] A. Zunger, Phys. Status Solidi B **224**, 727 (2001).
[21] A. Puzder, A. J. Williamson, J. C. Grossman, and G. Galli, J. Am. Chem. Soc. **125**, 2786 (2003); E. Degoli, G. Cantele, E. Luppi, R. Magri, D. Ninno, O. Bisi, and S. Ossicini, Phys. Rev. B **69**, 155411 (2004).
[22] S. Furukawa and T. Miyasato, Phys. Rev. B **38**, 5726 (1988).
[23] S. Lee, J. Sanchez-Dehesa, and J. D. Dow, Phys. Rev. B **32**, 1152 (1985); S. Richard, F. Aniel, and G. Fishman, J. Appl. Phys. **94**, 1795 (2003).
[24] J. B. Foresman, M. Head-Gordon, J. A. Pople, and M. J. Frish, J. Phys. Chem. **96**, 135 (1992).
[25] M. M. Francl, W. J. Pietro, W. J. Hehre, J. S. Binkley, M. S. Gordon, D. J. DeFrees, and J. A. Pople, J. Chem. Phys. **77**, 3654 (1982).
[26] E. W. Draeger, J. C. Grossman, A. J. Williamson, and G. Galli, J.

Chem. Phys. **120**, 10807 (2004).
[27] D. Bimberg, M. Grundmann, and N. N. Ledentsov, *Quantum Dot Heterostructures* (John Wiley & Sons Ltd., New York, 1999).
[28] C. S. Garoufalis, A. D. Zdetsis, and S. Grimme, Phys. Rev. Lett. **87**, 276402 (2001); I. Vasiliev, S. Ogut, and J. R. Chelikowsky, Phys. Rev. Lett. **86**, 1813 (2001).
[29] H. Asaoka, V. Cherepanov, and B. Voigtlander, Surf. Sci. **588**, 19 (2005).
[30] O. Akcakir, J. Therrien, G. Belomoin, N. Barry, J. D. Muller, E. Gratton, and M. Nayfeh, Appl. Phys. Lett. **76**, 1857 (2000).